Electronic Supplementary Material (ESI) for New Journal of Chemistry.
This journal is © The Royal Society of Chemistry and the Centre National de la Recherche Scientifique 2023

# Supporting Information

## Wet-chemical assisted synthesis of MnSe/ZnO nanostructures as low-resistance robust novel cathode material for advanced hybrid supercapacitors

Muhammad Zia Ullah Shah[1,2], Muhammad Sajjad[3**],Muhammad Sanaullah Shah[1,2], Muhammad Rahim[4] , Shams ur Rahman[5] ,Hongying Hou[1*]Afaq Ullah Khan[6] and A. Shah[2**]

[1]Faculty of Materials Science and Engineering, Kunming University of Science and Technology, Kunming 650093, China

[2]National Institute of Lasers and Optronics College, Pakistan Institute of Engineering and Applied Sciences, Nilore, Islamabad 45650, Pakistan

[3]College of Chemistry and Life Sciences, Zhejiang Normal University, Jinhua 321004, P. R China

[4]Department of Physics, International Islamic University, H10, Islamabad, Pakistan

[5]Department of Physics, COMSATS University Islamabad, Pakistan

[6]School of Chemistry and Chemical Engineering, Jiangsu University, 301 Xuefu Road Zhenjiang 212013, China

* Corresponding author. Faculty of Materials Science and Engineering, Kunming University of Science and Technology, Kunming 650093, China

**Corresponding author.

E-mail address: hongyinghou@kust.edu.cn (H. Hou), sajjadfisica@gmail.com (M. Sajjad) attashah168@gmail.com (A.Shah)

## 1. Morphology and structural analysis

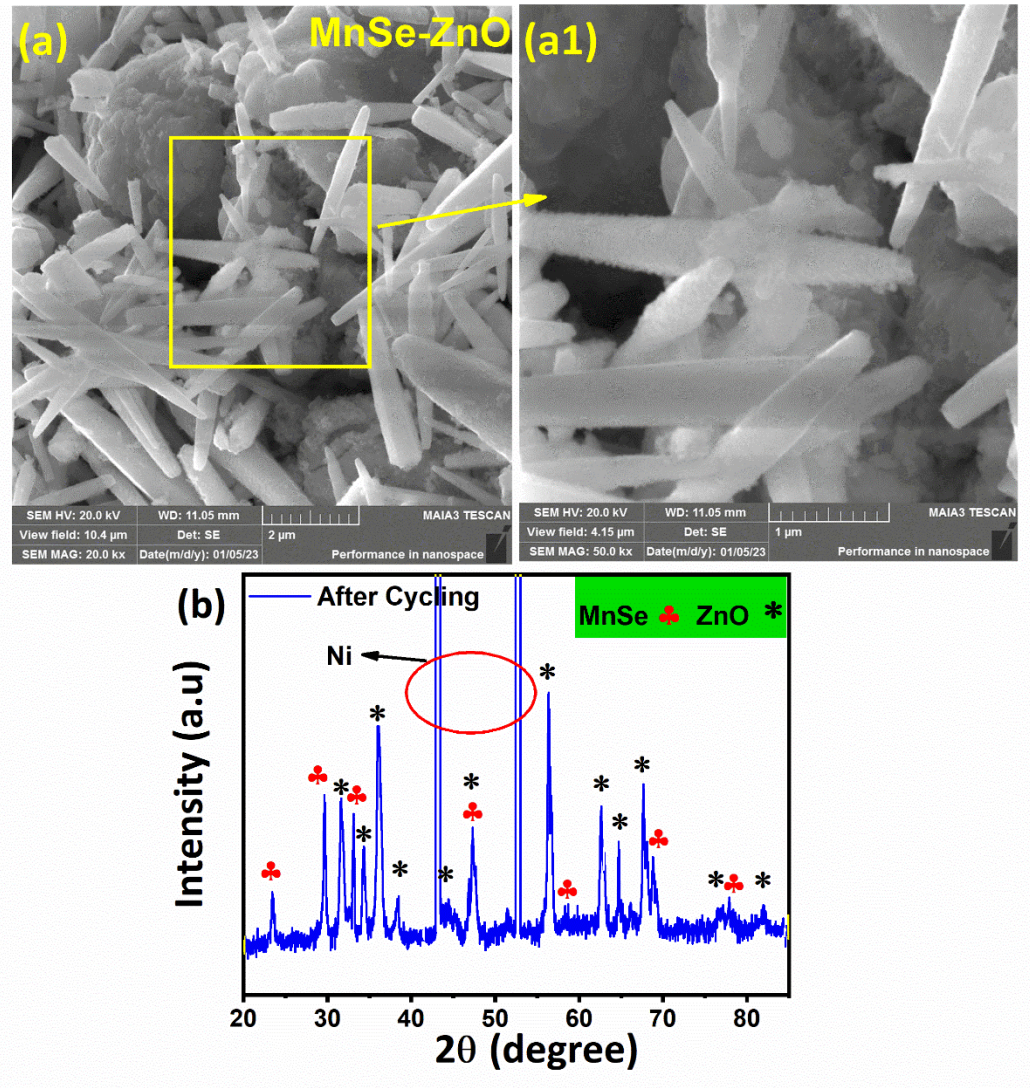


**Figure S1.** The FESEM micrograph after cycling stability (a, b), and (c) crystal structure after the cycling test.

## 2. XPS analysis

XPS spectra were produced to examine the surface chemistry and electronic states of the MnSe/ZnO composite. As shown in (**Fig. S2(a),** the whole survey spectrum shows the characteristic peaks of Se, Mn, Zn, O, and C. **Fig. S2(b)** showed two peaks are found in the high-resolution spectra of Mn, which have been assigned to Mn $2p_{1/2}$ (641.9 eV) and Mn $2p_{3/2}$ (653.2 eV). Furthermore, there are three distinct peaks in the deconvoluted spectrum of Se 3d: Se $3d_{1/2}$ (55.8 eV), Se $3d_{3/2}$ (54.7 eV), which confirms the existence of Se on the MnSe, and one satellite

peak at around 58.9 eV. **(Fig. S2c).** The high-resolution Zn 2p spectra reveal a doublet with binding energy peaks at 1024.5 eV and 1046.7 eV, corresponding to the Zn $2p_{3/2}$ and Zn $2p_{1/2}$ core levels, respectively **(Fig. S2) (d).** The calculated difference in binding energy (22.2 eV) from the XPS investigation indicates that Zn atoms were in the $Zn^{2+}$ oxidation state. **Figure S2(e),** which shows the high-resolution XPS spectrum of O1s, showed that the higher binding energy was (531.5 eV). The O2- ions on the hexagonal $Zn^{2+}$ ions in the wurtzite structure, which are surrounded by Zn atoms and contain the full complement of nearest-neighbor $O^{2-}$ ions, correspond to this binding energy. The powerful binding energies of Zn 2p and O 1s indicate the fabrication of pure ZnO materials by interacting with $Zn^{2+}$ and $O^{2-}$ ions in ZnO crystals to form Zn–O bonds. In addition, we examined and detected carbon peaks in the high-resolution spectra to confirm the existence of MnSe-ZnO in the composite **Fig. S2 (f).** The MnSe-ZnO composite shows two peaks, at 284.5 eV and 286.6 eV, that can be attributed to the C-C and O-C peaks, respectively. We can claim that the MnSe-ZnO composite was effectively synthesized because these findings are consistent with the XRD and Raman data.

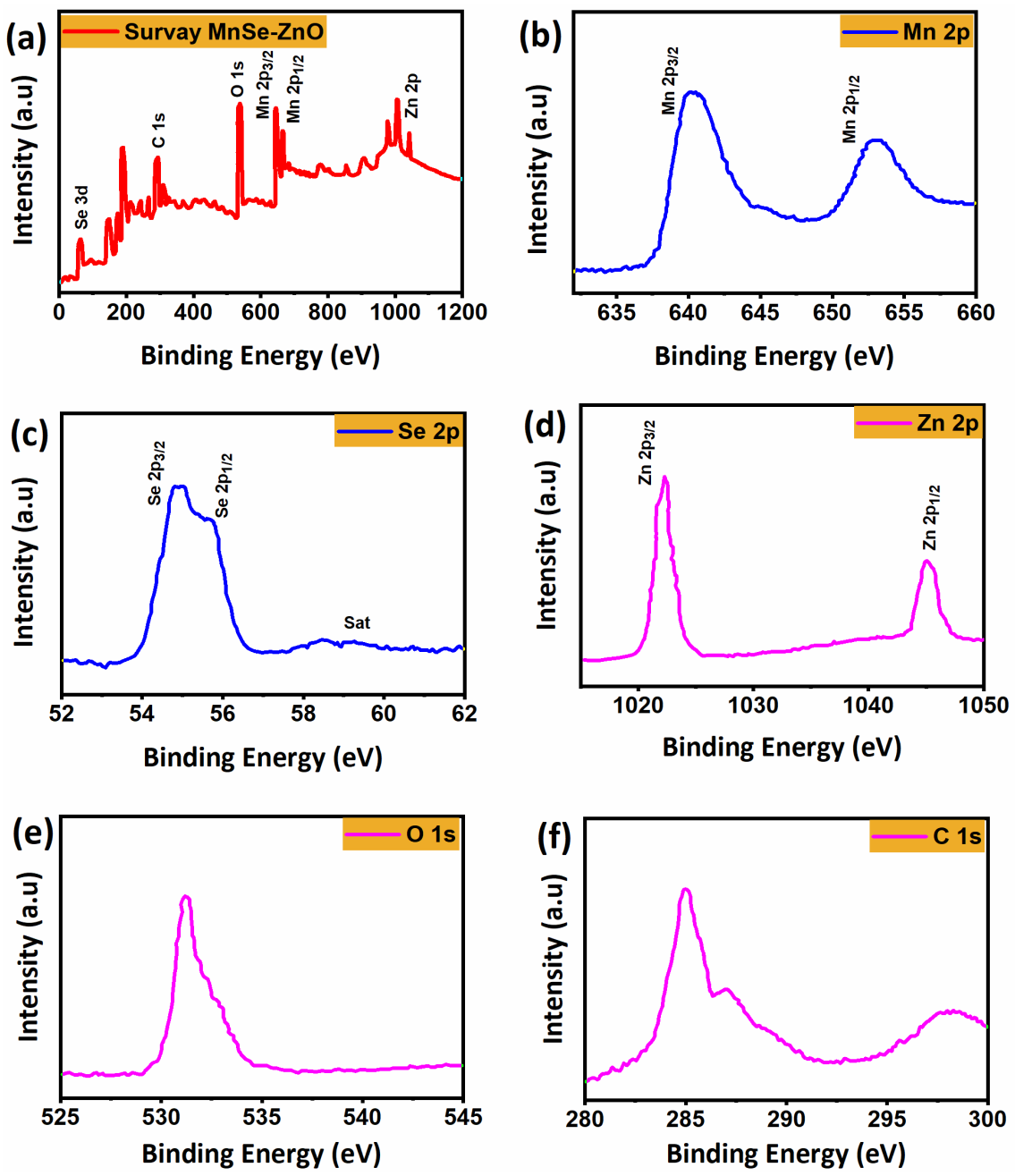


**Figure S2.** XPS spectrum of ZK-2 sample, (a) survey spectra, (b) Mn 2p, (c) Se 2p, (d) Zn 2p, (e) O 1s, and (f) C 1s.

## 3. Charge discharging

The GCD curves of the KT-3 electrode are provided in **Fig. S3a**. It was noticed that when the concentration of MnSe increases further, the capacitance decreases, as given in **Fig. S3b**. and the concentration of MnSe details added in the revised manuscript in the **table.1**

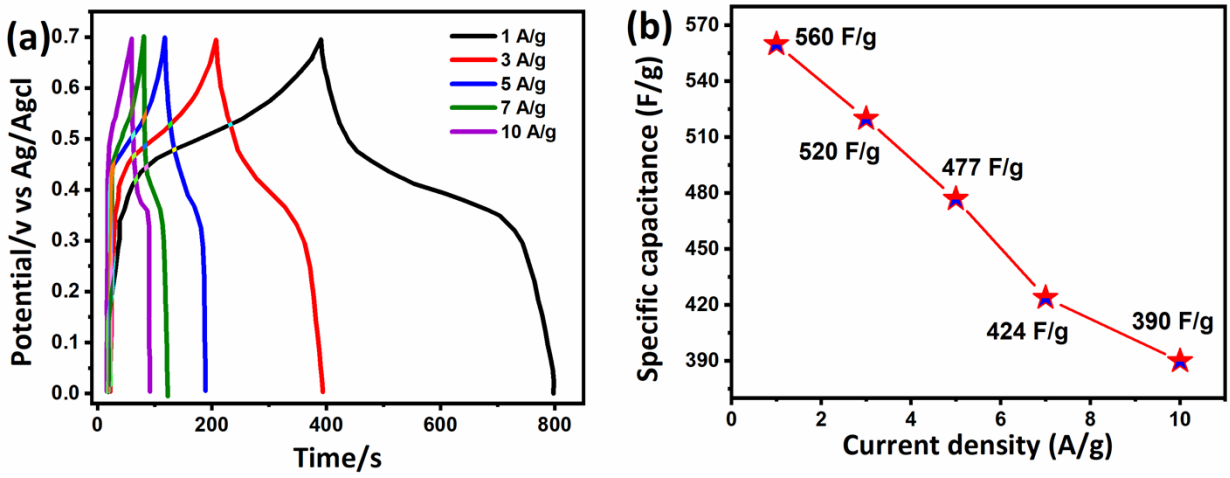


**Figure S3.** (a) GCD profile, and (b) capacitance plot of the ZK-3 electrode.

## 4. The Brunauer-Emmett-Teller (BET) for surface area

N2 adsorption/desorption isotherms were used to investigate further the porous surface area of the samples **(Fig. S4(a-d)).** Type IV isotherms confirmed the existence of mesopores in all four samples. The synthesized KT-2 composite used to have a BET surface area of 48.4 $m^2g^{-1}$, which was much greater than the values for KT-1 (42.7 $m^2g^{-1}$), and (35.8 $m^2g^{-1}$) and ZnO (28.3 $m^2g^{-1}$). The KT-2 sample has a high capacitance because it has a lot of surface area. This can be seen in the electrochemical analysis. The pore size distribution curves of Fe-SNC and SNC are shown in the inset of Figure S4 (a1-d1). KT-2 has a 27.8 nm pore size distribution, indicating mesoporosity with higher pore width, allowing for excessive ion transport during the intercalation/deintercalation process.

In contrast, ZnO, MnSe, and KT-1 have 23.5 nm, 24.7 nm, and 26.2 nm pores, respectively. These results demonstrate that the mesoporous nanostructures of the four samples contain a substantial surface area, which is required for the best electrochemical performance. The

BET analysis was also added in the revised manuscript in **supporting information (Section 4).**

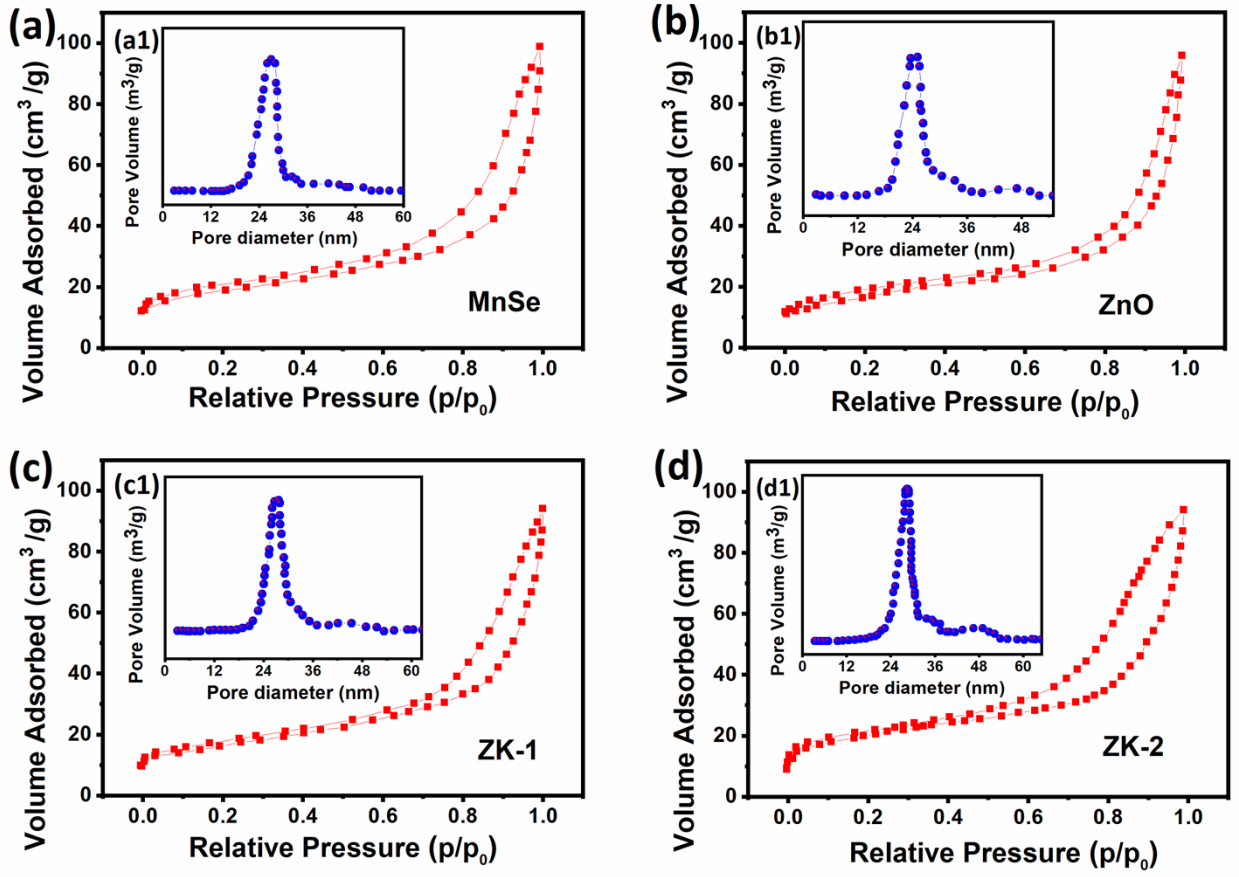


**Fig: S4** The Brunauer-Emmett-Teller (BET) surface area was determined using nitrogen adsorption/desorption isotherms, and the insets **(a1-d1)** show the associated pore-size distribution of the (a) and (b) ZnO and (c) KT-1 and (d) KT-2 samples.

The MnSe and ZnO bandgap energy is listed in Scheme 1. As seen, the ZnO has a higher Fermi level, meaning that the electrons will move from ZnO to MnSe with a lower Fermi level (as seen before contact), which leads to the former becoming positive and the latter bearing negatively charged. Whenever the Fermi levels of such components reach equilibrium, the influential band will begin at heterointerfaces automatically and cause the charge to be redistributed close to the interfaces. As a result, the electrons and holes gather close to the heterointerface and are divided from one another by a completely ionized depletion area, creating an inherent potential. Since this intrinsic potential, the heterostructure materials significantly conduct in the upward bias direction. However, the ZnO and MnSe utilise p-type and n-type with diverse reversibility that built

heterostructure [a, b]. The formation of heterostructure boosts the conduction of ions, and conductivity lowers the energy barriers, resulting in a synergistic effect.

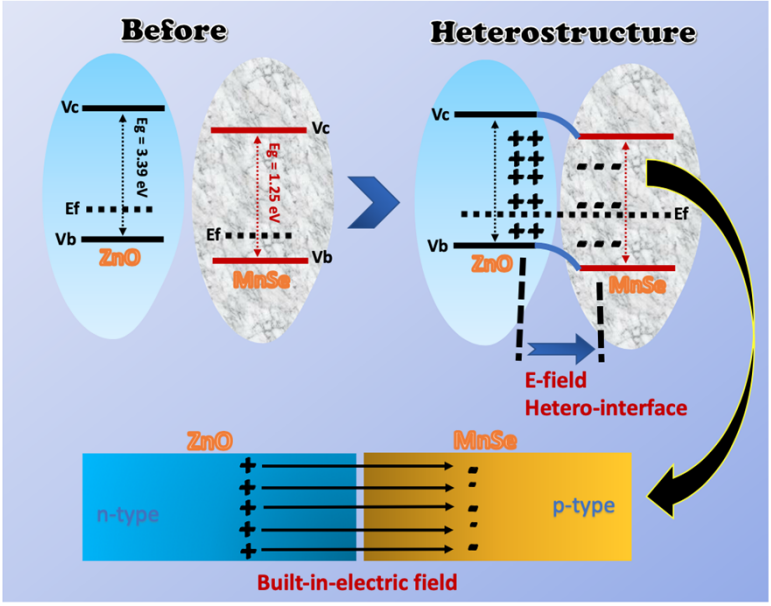


**Scheme 1.** The schematic of the energy storage mechanism in heterostructure between ZnO/MnSe composite electrode.

[a]. J. Ni, M. Sun, L. Li, Adv. Mater. 2019, 31, 1902603.

[b]. S. Wu, K. S. Hui, K. N. Hui, Adv. Sci. 2018, 5, 1700491.